Differential Analysis of *Saccharomyces cerevisiae* Mitochondria by Free Flow Electrophoresis*[S]

Hans Zischka‡§¶, Ralf J. Braun‡, Enrico P. Marantidis‡, Dietmute Büringer‖, Carsten Bornhövd**, Stefanie M. Hauck‡, Oliver Demmer‡, Christian J. Gloeckner‡, Andreas S. Reichert**, Frank Madeo‡‡, and Marius Ueffing‡§§

One major problem concerning the electrophoresis of mitochondria is the heterogeneity of mitochondrial appearance especially under pathological conditions. We show here the use of zone electrophoresis in a free flow electrophoresis device (ZE-FFE) as an analytical sensor to discriminate between different yeast mitochondrial populations. Impairment of the structural properties of the organelles by hyperosmotic stress resulted in broad separation profiles. Conversely untreated mitochondria gave rise to homogeneous populations reflected by sharp separation profiles. Yeast mitochondria with altered respiratory activity accompanied by a different outer membrane proteome composition could be discriminated based on electrophoretic deflection. Proteolysis of the mitochondrial surface proteome and the deletion of a single major protein species of the mitochondrial outer membrane altered the ZE-FFE deflection of these organelles. To demonstrate the usefulness of ZE-FFE for the analysis of mitochondria associated with pathological processes, we analyzed mitochondrial fractions from an apoptotic yeast strain. The *cdc48*^{S565G} strain carries a mutation in the *CDC48* gene that is an essential participant in the endoplasmic reticulum-associated protein degradation pathway. Mutant cells accumulate polyubiquitinated proteins in microsomal and mitochondrial extracts. Subsequent ZE-FFE characterization could distinguish a mitochondrial subfraction specifically enriched with polyubiquitinated proteins from the majority of non-affected mitochondria. This result demonstrates that ZE-FFE may give important information on the specific properties of subpopulations of a mitochondrial preparation allowing a further detailed functional analysis. ***Molecular & Cellular Proteomics 5:2185–2200, 2006.***

From the Institutes of ‡Human Genetics and §Toxicology, GSF-National Research Center for Environment and Health, 85764 Munich-Neuherberg, Germany, ‖Department of Systems and Computational Neurobiology, Max Planck Institute for Neurobiology, 82152 Martinsried, Germany, **Adolf-Butenandt-Institute for Physiological Chemistry, Ludwig-Maximilians University Munich, 81377 Munich, Germany, ‡‡Institute of Molecular Biosciences, University of Graz, Graz A-8010, Austria, and §§Institute for Human Genetics, Technical University Munich, 81675 Munich, Germany

Received, April 5, 2006, and in revised form, August 11, 2006

Published, MCP Papers in Press, August 17, 2006, DOI 10.1074/mcp.T600018-MCP200

Fundamental cellular processes are linked to mitochondria, the powerhouse of the cell (1). In addition to their anabolic and metabolic importance, higher eukaryotic life and (programmed) cell death (*i.e.* apoptosis) involve the considerable participation of these organelles (2). Life expectancy is also directly linked to mitochondrial well being because longevity correlates with low mitochondrial production of reactive oxygen species and low accumulation of mutations in mitochondrial DNA (3). Consequently mitochondria are the focus of ongoing studies involving a multitude of biochemical and physical approaches (2, 4, 5). One major issue here is the considerable heterogeneity in mitochondrial appearance and function due to pathology. Using electron microscopy, several studies report mitochondria with swollen and misshapen membranes in association with various diseases (6, 7). One approach to analyze such alterations is the study of the mitochondrial proteome (8), which aims first at a quantitative description followed by dynamic changes in expression of the mitochondrial proteome. Studies on mitochondria isolated from human (9), rodent (10), and plant tissues (11) and especially from yeast (12) have substantially contributed to our knowledge of the mitochondrial proteome over the past years (8). It remains to be determined, however, whether current methodological approaches are capable of thoroughly detecting and identifying specific pathological alterations in a heterogeneous mitochondrial population.

We recently demonstrated that isolation procedures for mitochondria from *Saccharomyces cerevisiae*, including zone electrophoresis in a free flow electrophoresis device (ZE-FFE),[1] yielded organelles with a high degree of purity and consequently improved subsequent proteome analyses (13, 14), thus proposing ZE-FFE as a very useful tool for effective mitochondrial purification. Introduced over 40 years ago (15), ZE-FFE methods and devices have since been considerably

[1] The abbreviations used are: ZE-FFE, zone electrophoresis in a free flow electrophoresis device; 2-DE, two-dimensional gel electrophoresis, ER, endoplasmic reticulum, ERAD, ER-associated protein degradation; Glc mitochondria, mitochondria isolated from yeast grown in glucose medium; Lac mitochondria, mitochondria isolated from yeast grown in lactate medium; ΔTOM70 mitochondria, mitochondria isolated from a TOM70 deletion strain grown in lactate medium; YPD, glucose medium; YPGal, galactose medium; EM, electron microscopy; ACTH, adrenocorticotropic hormone; CE, capillary electrophoresis.

improved. However, the basic principle has remained unvaried: charged particles (*e.g.* mitochondria) are injected into a laminar buffer stream, deflected by a perpendicular electrical field, and collected at the end of the separation chamber. Partition of mitochondria from contaminants is therefore a consequence of the deflection properties of mitochondria, which differ sufficiently from those of the separated particles. This implies that affecting these properties will alter the migration behavior of mitochondrial populations in ZE-FFE, thus providing the unique possibility of using this technique as an analytical tool.

In this study we assessed the potential of ZE-FFE as analytical sensor to discriminate between different yeast mitochondrial populations. We observed that, in correlation with specific structural properties, appearance, and surface proteomes of analyzed organelles, characteristic ZE-FFE separation profiles were evident. Disrupted organelles demonstrated profiles with broad peaks of low signal to noise ratio, thus allowing quality assessment of a given organelle preparation. A broad peak was also observed with osmotically stressed mitochondria. Moreover physiological different mitochondrial populations could be discriminated by ZE-FFE deflection whereby deletion of a single major protein species in the mitochondrial outer membrane led to altered ZE-FFE deflection of the entire organelle sample. The relationship between the resultant ZE-FFE separation profile and outer mitochondrial membrane composition could be further demonstrated by proteolytic cleavage of the mitochondrial surface proteome.

To assess the benefits of ZE-FFE as a suitable application in the differential analysis of distinct mitochondrial populations isolated from pathophysiological cellular conditions, we compared mitochondria isolated from the apoptotic yeast strain *cdc48*^{S565G} (16) to mitochondria isolated from a yeast strain expressing wild-type Cdc48p. Cdc48p is an important participant in the ubiquitin-dependent ER-associated protein degradation pathway (17–19). Upon mutation of a single amino acid residue in this protein (Cdc48p-S565G), cells accumulate polyubiquitinated proteins. Interestingly we observed strong polyubiquitination not only in microsomes but also in mitochondria. Using ZE-FFE, we showed that only a subset of the mitochondria from the apoptotic *cdc48*^{S565G} strain was affected by polyubiquitination and that the major part of these organelles appeared to remain unaltered. These results demonstrate that ZE-FFE may give important information on the specific properties of subpopulations of a given mitochondrial preparation, which so far was considered to be homogeneous.

EXPERIMENTAL PROCEDURES

Isolation of Yeast Mitochondria and Microsomes—*S. cerevisiae* strains BY4741 and Y07244 (genotype *BY4741*; *MAT a*; *his3Δ1*; *leu2Δ0*; *met15Δ0*; *ura3Δ0*; *YNL121c*::*kanMX4*) were grown to logarithmic phase in YPD (1% yeast extract, 2% Bacto-peptone, 4% glucose (Glc) or lactate (Lac) media (3‰ yeast extract, 1‰ Glc, 1‰ NH_4Cl, 1‰ KH_2PO_4, 1.1‰ $MgSO_4$, 0.5‰ NaCl, 0.5‰ $CaCl_2$, 2% lactate, 0.3‰ $FeCl_3$). Cells were harvested in logarithmic phase, and mitochondria were isolated by differential centrifugation (13, 20), resuspended in SET buffer (0.25 M sucrose, 1 mM EDTA, 10 mM Tris/HCl, pH 7.4, 1 mM PMSF) at 5–20 mg/ml, shock frozen with liquid nitrogen, and stored at −80 °C until further use.

S. cerevisiae mutant strains KFY437 (*cdc48*^{S565G}) and wild-type KFY417 (21) were used for the comparisons of polyubiquitinated mitochondrial fractions. Cells were grown at least 36 h at 28 °C in baffled flasks on YPGal (1% yeast extract, 2% Bacto-peptone, 4% galactose). Cultures were sedimented and washed twice in YPD. For induction of apoptosis, washed YPGal cultures were then grown in YPD in baffled flasks at 28 °C until stationary phase and subjected to heat shock at 37 °C for 4 h (16, 22). Mitochondria were isolated from these stationary cultures as described above. Microsomes were collected by ultracentrifugation (177,000 × *g* for 90 min at 4 °C) from the supernatant of the first mitochondrial sedimentation.

Mitochondrial Respiration Measurements—Mitochondrial oxygen consumption was measured as described previously (23) in a 1.5-ml thermostatically controlled cuvette equipped with a Clark oxygen electrode connected to a microcomputer (both Consort, Turnhout, Belgium) at 27 °C. Basal medium was 0.65 M mannitol, 10 mM Tris maleate, pH 6.7, 3 mM Tris phosphate; respiration was initiated with ethanol.

Mitochondrial Surface Proteolysis—Surface proteolysis of mitochondria was conducted by mild tryptic treatment as published previously (24). Briefly mitochondria were suspended in ZE-FFE separation buffer at a concentration of 5 mg/ml. Trypsin (sequence grade, Promega) was added to reach a final concentration of 2 μg/ml. After a 15-min incubation on ice, reactions were stopped with 1 mM PMSF treatment for 5 min. Samples were washed (16,100 × *g* for 12 min at 4 °C) and applied to ZE-FFE.

ZE-FFE Analysis—Different mitochondrial populations were subjected to zone electrophoretic separation at the cathodal side into a free flow electrophoresis apparatus (Weber GmbH, Planegg, Germany); for reviews on this method, see Ref. 25 or 26.

Experiments were carried out according to our previous report (13) with the following modifications. (i) EDTA was omitted from the circuit electrolytes, electrolyte stabilizers, and separation media. (ii) All buffers were cooled on ice during separation to avoid thermal gradients. (iii) Mitochondrial samples were washed once in separation media (16,100 × *g* for 12 min at 4 °C) and applied to ZE-FFE at concentrations of 1–5 mg/ml with a sample flow rate of 1–2 ml/h. (iv) Pulsing of the sample stream upon introduction in the separation chamber was carefully avoided. (v) All ZE-FFE comparisons between Lac and Glc mitochondria were performed in separation buffer (10 mM acetic acid, 10 mM triethanolamine, pH 7.4) containing 0.5 M sucrose because these slightly hyperosmotic conditions were found to stabilize Glc mitochondria isolated from cells in logarithmic phase (see "Results"). ZE-FFE comparisons between Lac mitochondria and mitochondria with deleted TOM70 protein as well as comparisons between mitochondria from strains expressing wild-type Cdc48p or mutant Cdc48p-S565G were done in separation buffer containing 0.3 M sucrose. (vi) Electrophoresis was performed in horizontal mode at 5 °C with a total flow rate of 400 ml/h within the separation chamber and at a voltage of 750 V. (vii) Fractions were collected in 96-well plates, and the distribution of resolved particles was monitored at a wavelength of 260 nm with a Synergy™ HT microplate reader (Bio-Tek Instruments, Bad Friedrichshall, Germany). (viii) Mitochondria from ZE-FFE fractions were concentrated by centrifugation at 4 °C (12 min at 16,100 × *g*). The pellets were shock frozen in liquid nitrogen and used for either electron microscopy (EM) or protein analysis.

ZE-FFE Validation and Control Experiments—To ensure constant separation conditions during the ZE-FFE analysis of different mitochondrial populations, control experiments and routine tests of the ZE-FFE apparatus were conducted.

The apparatus was set up on a daily basis to avoid abrading the instrument seals. Uniformity of laminar buffer flow was inspected daily

according to the manufacturer's recommendations, and flow velocities of all buffers were routinely controlled, and disturbances (*e.g.* entrapped air bubbles) were carefully avoided.

Cellular organelles (especially Glc mitochondria) have a certain tendency toward aggregation, which might form irreversible "clots" and might severely affect their electrophoretic analysis (27, 28). An advantage of the ZE-FFE technique is that such white, mitochondria-derived clots are clearly visible in the separation chamber, and if they occur, frequently form at the sample entry. Consequently a regular visual inspection of the separation chamber during each analysis was done to control for and avoid such a considerable mitochondrial aggregation. Several conditions, such as increased ionic strength and/or the presence of divalent ions such as Mg^{2+} or Ca^{2+}, are known to facilitate mitochondrial aggregation (27). Thus, EDTA was present during the preceding mitochondrial isolation procedure. In the subsequently used electrophoresis buffers EDTA was absent; however, ultra pure water was used for these buffers to keep ionic strength as low as possible. Careful suspension of mitochondrial samples was done on ice with the avoidance of strong shear forces, which are known to facilitate organelle damage and subsequent "clotting" (20). As further remedy against mitochondrial aggregation and if clotting was visible in the mitochondrial starting samples for ZE-FFE, a short centrifugation step (500 × *g* for 3 min at 4 °C) was used to remove aggregates. Separation tests with yeast mitochondria were carried out extensively and used to verify constant separation conditions during the ZE-FFE analysis (>5 h).

Comparisons of mitochondrial populations, *e.g.* Glc *versus* Lac mitochondria, were done consecutively on the same day and under identical conditions (voltage, buffer composition, buffer and sample velocity, and temperature). Samples were applied at comparable concentrations in alternating order. From each sample, several separation profiles were recorded (usually over a period of 1 h) to ensure time stability and exclude drifts in separation conditions.

We assessed the consistency of the various ZE-FFE deflection behaviors representing the diverse mitochondrial populations. Here independent mitochondrial preparations, *i.e.* Glc ($n = 7$), Lac ($n = 7$), and ΔTOM70 ($n = 5$), were investigated. Very similar results were obtained, *e.g.* Glc and Lac comparisons ($n = 7$) typically showed differences in deflection of two to three fractions (Fig. 3). This finding was further confirmed by independent analysis using another FFE device as well as with Glc and Lac mitochondria isolated from another yeast strain (W303; data not shown). Moreover similar ZE-FFE results were obtained from Lac and ΔTOM70 mitochondria ($n = 12$) comparisons, *i.e.* differences in deflection of one to two fractions (Fig. 7*B*). ZE-FFE comparisons of mitochondrial preparations isolated from wild-type and *cdc48*^{S565G} strains under apoptotic conditions ($n = 4$) were done from two independent preparations each (Fig. 8*C*).

Preparation of Outer Mitochondrial Membranes—Outer mitochondrial membranes were isolated according to various reports (29–32) with the following modifications. Mitochondria were isolated from strains BY4741 grown in YPD or Lac media and Y07244 grown in Lac media. To achieve higher organelle purity, separation was done by sucrose density gradient centrifugation (33, 34). Purified mitochondria (~20 mg) were washed (16,100 *g* for 12 min at 4 °C) and resuspended in 1.5 ml of ZE-FFE separation buffer containing 0.5 M sucrose for mitochondria isolated from cells grown on Glc or 0.3 M sucrose for cells grown on Lac. A small aliquot was used as whole organelle ZE-FFE control. The remainder received 15 ml of ZE-FFE separation buffer containing protease inhibitor mixture (Roche Applied Science) but without sucrose to produce hypo-osmotic swelling and were incubated for 25 min on ice with stirring. Subsequently hyperosmotic contraction was induced by adding 8 ml of ZE-FFE separation buffer containing 2 M sucrose and incubating for 10 min on ice. Osmotically stressed organelles were collected (40,000 × *g* for 30 min at 4 °C) and resuspended in 1 ml of ZE-FFE separation buffer (containing 0.5 or 0.3 M sucrose for Glc or Lac mitochondria, respectively). Samples were homogenized (10 strokes) with a glass homogenizer, and mitochondrial debris was removed by centrifugation (16,100 × *g* for 10 min at 4 °C). The supernatants, containing the outer membranes, were subsequently applied to ZE-FFE. Each separation was monitored at 260 or 240 nm. Fractions migrating similarly to the whole organelle control were collected and diluted 1–3-fold with ZE-FFE separation buffer containing protease inhibitor mixture (Roche Applied Science) but without sucrose. Outer membranes were collected by ultracentrifugation (166,000 × *g* for 45 min at 4 °C) and stored at −80 °C until further study (electron microscopy and protein analysis).

Analysis of Mitochondrial Membrane Proteins—Membrane protein extracts were obtained by standard alkaline carbonate extraction (35) of Glc or Lac mitochondria followed by solubilization in 1% dodecylmaltoside or 1% Triton X-100. Extracts were resolved by two-dimensional gel electrophoresis (2-DE) as described previously (13) whereby 1% dodecylmaltoside or 1% Triton X-100 was used during isoelectric focusing and that resulted in nearly identical separation patterns. Typically sample load was 50 μg of protein extract on 24-cm IPG (pH 3–10 non-linear, GE Healthcare) followed by SDS-PAGE on 9–14% T gradient gels (13). Separated proteins were visualized by silver staining (36), and gels were digitized using a GS 800 densitometer (Bio-Rad). Three representative gels from each protein extract condition, Glc and Lac mitochondria, combined to produce respective "raw master gels" were qualitatively compared using the Z3 software package (Fig. 2*B*) and quantitatively evaluated with Proteomweaver software Version 2.2 (Definiens, Munich, Germany) (Supplemental Table 1 and Supplemental Fig. 1B). Protein extracts of outer mitochondrial membranes were separated by SDS-PAGE according to Laemmli (37), and protein bands were visualized by either silver staining (36) or colloidal Coomassie (38).

Selected protein spots from 2-DE or SDS-PAGE were excised, destained, and processed by proteolysis (36, 39, 40). Peptide mixtures originating from proteins from 2-DE analysis were analyzed on a MALDI-TOF/TOF tandem mass spectrometer (ABI 4700 Proteomics Analyzer, Applied Biosystems), and peptide mixtures originating from proteins from SDS-PAGE were analyzed on a Bruker Reflex III mass spectrometer equipped with a Scout 384 inlet (Bruker-Daltonik). Data acquisition, processing, and subsequent database search was done as follows.

(i) Raw data for protein identification from 2-DE spots were obtained on the ABI 4700 Proteomics Analyzer (Applied Biosystems) and analyzed by GPS Explorer 2.0 software (Applied Biosystems). For positive ion reflector mode spectra 2500 laser shots were averaged and processed with external calibration based on a peptide mixture of angiotensin II acetate with monoisotopic mass of $[M + H]^+$ ion signal at 1046.54 Da, substance P (1347.74 Da), bombesin (1619.82 Da), and ACTH-(18–39) (2465.20 Da). All calibration peptides were obtained from Sigma). No smoothing or background subtraction was applied to the averaged MS spectra. Monoisotopic peak masses were automatically determined within the mass range 800–4000 kDa with a signal to noise ratio minimum set to 5 and a local noise window width of *m/z* 200. Up to seven of the most intense ion signals with signal to noise ratio above 30 were selected as precursors for MS/MS acquisition excluding common trypsin autolysis peaks and matrix ion signals. In MS/MS positive ion mode 4000 spectra were averaged, collision energy was 1 kV, collision gas air was at a pressure of 1.6×10^{-6} torrs, and default calibration was set. Monoisotopic peak masses were automatically determined with a signal to noise ratio minimum set to 10 and a local noise window width of *m/z* 200. Combined peptide mass fingerprinting and MS/MS queries were performed using the MASCOT® Database search engine version 1.9 (41) (Matrix Science Ltd.) embedded into GPS Explorer software

TABLE I

Identified mitochondrial membrane proteins extracted by sodium carbonate treatment from Lac/Glc mitochondria and separated by 2-DE (Fig. 2B and Supplemental Fig. 1)

Raw data for protein identification from 2-DE spots were obtained on the ABI 4700 Proteomics Analyzer and analyzed by GPS Explorer 2.0 software. Quantitative data regarding the 2-DE analysis of the selected proteins are listed in Supplemental Table 1. Further information regarding protein identification by the MS analysis is listed in Supplemental Table 2.

Spot no.	Swiss-Prot identifier	Protein name	Mitochondrial membrane[a]	Molecular mass[b]	pI[c]	Peptide count[d]	Protein score[e]	SC[f]	Intensity coverage[g]	MS/MS spectra[h]
				Da				%	%	
1	TOM70_YEAST	Mitochondrial import receptor subunit TOM70	OM	70,251	5.24	13	137	27	26.5	1
2	DLD1_YEAST	D-Lactate ferricytochrome *c* oxidoreductase	IM	65,935	6.37	23	351	51	35.7	2
3	DLD1_YEAST	D-Lactate ferricytochrome *c* oxidoreductase	IM	65,935	6.37	17	244	40	32.9	2
4	DLD1_YEAST	D-Lactate ferricytochrome *c* oxidoreductase	IM	65,935	6.37	12	89	28	18.6	0
5	DHSA_YEAST	Succinate dehydrogenase	IM	70,812	7.14	18	349	44	46.7	3
6	DHSA_YEAST	Succinate dehydrogenase	IM	70,812	7.14	17	320	33	42.7	3
7	DHSA_YEAST	Succinate dehydrogenase	IM	70,812	7.14	14	190	36	30.4	2
8	OM45_YEAST	Mitochondrial outer membrane 45-kDa protein	OM	44,553	8.55	18	405	44	28.3	4
9	OM45_YEAST	Mitochondrial outer membrane 45-kDa protein	OM	44,553	8.55	15	315	41	23.4	3
10	UQCR1_YEAST	Ubiquinol-cytochrome-*c* reductase complex core protein I	IM	50,254	6.77	10	213	30	31.3	2
11	UQCR2_YEAST	Ubiquinol-cytochrome-*c* reductase complex core protein II	IM	40,510	7.67	14	380	45	45.3	4
12	MCR1_YEAST	NADH-cytochrome b_5 reductase	OM	34,174	8.65	20	582	78	37.4	6
13	MCR1_YEAST	NADH-cytochrome b_5 reductase	OM	34,174	8.65	16	383	73	27.3	3
14	MPCP_YEAST	Mitochondrial phosphate carrier protein	IM	32,962	9.35	16	684	56	70.2	6
15	VDAC1_YEAST	Outer mitochondrial membrane protein porin1	OM	30,393	7.68	19	777	87	69.3	7
16	VDAC1_YEAST	Outer mitochondrial membrane protein porin1	OM	30,393	7.68	18	734	75	66.2	7
17	VDAC1_YEAST	Outer mitochondrial membrane protein porin1	OM	30,393	7.68	11	470	59	52.0	6
18	CY1_YEAST	Cytochrome c_1	IM	34,261	8.22	7	135	20	22.2	1
19	CY1_YEAST	Cytochrome c_1	IM	34,261	8.22	7	202	20	32.6	2
20	CY1_YEAST	Cytochrome c_1	IM	34,261	8.22	6	74	20	14.0	0
21	COX5A_YEAST	Cytochrome *c* oxidase polypeptide Va	IM	17,130	9.82	6	243	45	18.2	3
22	COX13_YEAST	Cytochrome *c* oxidase polypeptide VIa	IM	15,069	7.9	5	117	37	22.7	2
23	UCR7_YEAST	Ubiquinol-cytochrome-*c* reductase complex 14-kDa protein	IM	14,613	5.62	8	288	67	35.5	4

[a] Protein localization: IM, inner mitochondrial membrane; OM, outer mitochondrial membrane.

[b] Theoretical molecular mass of the identified protein (in daltons).

[c] Theoretical isoelectric point of the identified protein.

[d] Number of peptides that match identified protein.

[e] Probability-based MOWSE score (41) as given by MASCOT; scores >66 are significant ($p < 0.05$) for this analysis (search with combined peptide mass fingerprinting and MS/MS data).

[f] Sequence coverage, expressed as number of amino acids spanned by the assigned peptides divided by sequence length, given in percent.

[g] Intensity coverage, expressed as cumulative intensity of the peaks assigned to the hit divided by the cumulative intensity of all peaks of respective spectrum, given in percent.

[h] Number of MS/MS spectra obtained for the identified protein; only MS/MS spectra with scores >31 were considered.

(Applied Biosystems) on the Swiss-Prot database (version 20051206; 201,594 sequences; 73,123,101 residues) with the following parameter settings: 65 ppm mass accuracy, trypsin cleavage, one missed cleavage allowed, carbamidomethylation set as fixed modification, oxidation of methionines allowed as variable modification, MS/MS fragment tolerance set to 0.3 Da, and minimum ion score confidence interval for MS/MS data set to 98.5%. A protein was regarded as identified if the probability based MOWSE score (42) was significant

TABLE II

Identified outer mitochondrial membrane proteins from Lac/Glu mitochondria separated by SDS-PAGE (Fig. 6A)

Raw data were obtained on a Bruker Reflex III MALDI-TOF instrument and were processed and analyzed by the Bruker-Daltonik software X-Tof 5.1.0. Annotated spectra of the identified proteins are given in Supplemental Fig 2.

Sample	Swiss-Prot identifier	Accession number	Molecular mass[a]	Peptide count[b]	Protein score[c]	SC[d]	Intensity coverage[e]	Unmatched peptides[f]	Score of next non-homologue hit
			Da			%	%		
Band 1	TOM70_YEAST	P07213	70,079	14	172	36.8	76.7	29	65
Band 2	OM45_YEAST	P16547	44,553	32	287	63.4	70.1	23	55
Band 3	VDAC1_YEAST	P04840	30,278	15	139	62.4	66.1	36	56

[a] Theoretical molecular mass of the identified protein (in daltons).

[b] Number of peptides that match identified protein.

[c] Probability-based MOWSE score (41) as given by MASCOT; scores >67 are significant ($p < 0.05$) for this analysis.

[d] Sequence coverage, expressed as number of amino acids spanned by the assigned peptides divided by sequence length, given in percent.

[e] Intensity coverage, expressed as cumulative intensity of the peaks assigned to the hit divided by the cumulative intensity of all peaks of respective spectrum, given in percent.

[f] Number of unmatched peptides.

(protein scores greater than 66 were significant, $p < 0.05$), if the matched peptide masses were abundant in the spectrum, and if the theoretical masses of the significant hit fit the experimentally observed values. Single MS/MS spectra were only considered with MOWSE score greater than 31. A comprehensive list of the relevant details for the mass spectrometric identifications is given in Table I, and additional information on the associated MS/MS analysis is listed in Supplemental Table 2.

(ii) Raw data obtained on the Bruker Reflex III instrument were processed and analyzed by the Bruker-Daltonik software X-Tof 5.1.0 as described before (40). The instrument was externally calibrated using angiotensin II acetate (1046.54 Da), substance P (1347.74 Da), bombesin (1619.82 Da), and ACTH-(18–39) (2465.20 Da). 400 single spectra were combined for each sample; combined spectra where then smoothed, and background was subtracted (default settings in X-Tof 5.1.0). All monoisotopic peaks in the spectra were assigned manually using the centroid peak picking mode (X-Tof 5.1.0). Database searches were done using the MASCOT Database search engine version 2.1 (41) (Matrix Science Ltd.). Parameter settings were: 150 ppm mass accuracy, trypsin cleavage, one missed cleavage allowed, and oxidation of methionines allowed as variable modification. No limitations regarding the molecular weight or for specific peptide masses were set. The search was done against all entries of Swiss-Prot (version 50.0; 290,834 sequences; 140,379,986 residues). A protein was regarded as identified (Table II) if the probability-based MOWSE score (42) was significant (protein scores greater than 67 were significant, $p < 0.05$) and if the matched peptide masses were abundant in the spectrum (intensity coverage >50%). A comprehensive list of the relevant details for the mass spectrometric identifications is given in Table II, and the annotated spectra of the identified proteins are given in Supplemental Fig 2.

Immunoblotting of whole mitochondrial protein extracts resolved by SDS-PAGE was carried out according to Towbin *et al.* (43) using polyclonal antisera against TOM70, VDAC1, AAC2, and the 40-kDa microsomal protein and monoclonal antibodies against DPM1 and ubiquitin. Electron microscopy of the diverse mitochondrial preparations and subfractions was done as recently reported (13).

RESULTS

Mitochondria are delicate structures, and harsh isolation procedures, such as prolonged homogenization of starting cells or tissue, impose strong shear forces leading to disruption of mitochondrial membranes (20). Another destabilizing constraint lies in the dynamic nature of the mitochondrial proteome under various (patho)physiological conditions (44, 45). We show here that *S. cerevisiae* mitochondrial populations originating from different biological conditions or experimental manipulation are clearly distinguishable by ZE-FFE.

ZE-FFE Allows the Differential Analysis of Mitochondrial Populations—The use of ZE-FFE as an analytical sensor for the heterogeneity of a given mitochondrial population can be demonstrated by comparing yeast mitochondria obtained through different isolation procedures, *i.e.* by differential centrifugation in the presence or absence of an additional sucrose density gradient centrifugation (Fig. 1). Sucrose density gradients impose strong osmotic pressure on mitochondria due to the limited permeability of the inner mitochondrial membrane toward sucrose (46, 47) and induce heterogeneity in shape and extent of matrix condensation (Fig. 1*A*, *left panel*). This is paralleled by markedly different ZE-FFE separation profiles (Fig. 1*A*, *right panel*) in contrast to mitochondria not additionally purified by sucrose density gradient centrifugation (Fig. 1*B*, *right panel*). Whereas the latter gave rise to a sharp peak containing mitochondria that appeared highly homogeneous (Fig. 1*B*, *left panel*), osmotically stressed mitochondria typically showed broader peaks. In addition, in the displayed example, a strong tailing toward the anode was detected (Fig. 1, *cf. A* and *B*, *right panels*).

If differences between organelle populations based on electrophoretic deflection can be detected by ZE-FFE, we then asked whether this method would also discriminate mitochondria isolated from different cellular backgrounds. We addressed this question by analyzing mitochondria isolated from yeast in logarithmic growth phase cultivated on different carbon sources, *i.e.* Lac *versus* Glc, conditions that force cellular shifts of homeostatic metabolism to respiration or respirofermentation, respectively (48). Whereas mitochondria isolated from respiratory cells (termed "Lac mitochondria") retain their ability to consume oxygen upon substrate addition (Fig. 2*A*),

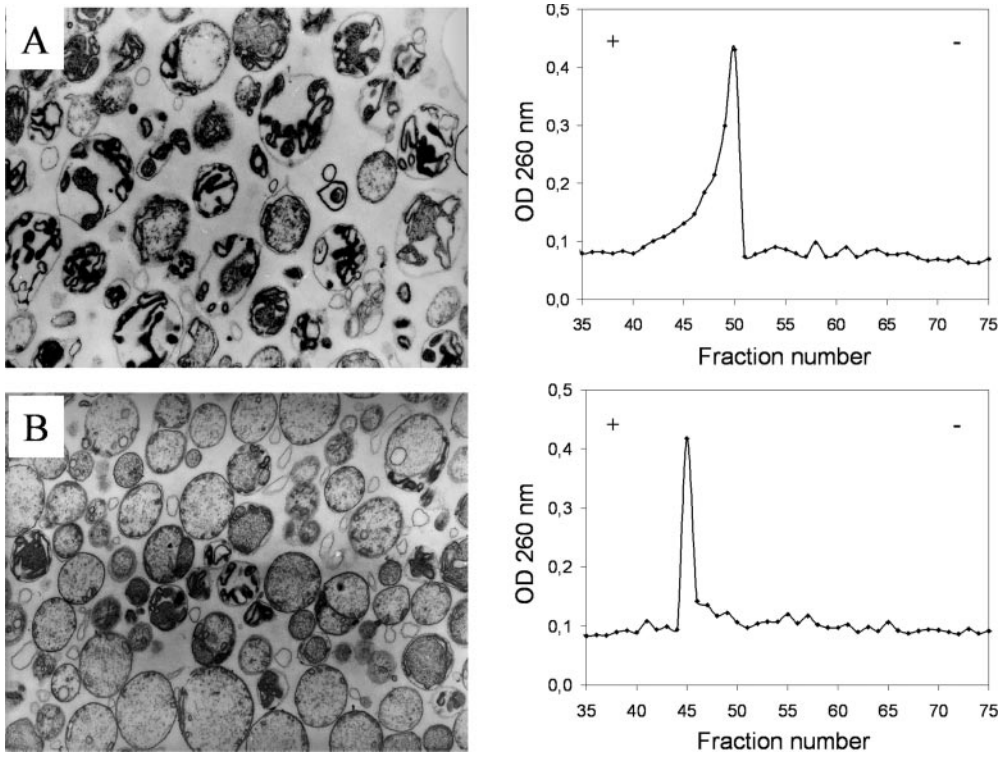

FIG. 1. **Monitoring the effect of sucrose density gradient purification of yeast mitochondria by ZE-FFE.** *A*, electron micrograph (*left panel*; *magnification*, 32,000) of mitochondria isolated from yeast grown on lactate media. Organelles were isolated by differential centrifugation and further purified by sucrose density gradient centrifugation. Subsequent ZE-FFE analysis (*right panel*) revealed the mitochondrial heterogeneity by a broad main peak (anode, +; cathode, −). *B*, electron micrograph of mitochondria isolated by differential centrifugation showing homogeneous organelles (*left panel*) and demonstrating a sharp main peak in the ZE-FFE separation profile (*right panel*).

mitochondria isolated from fermenting cells (termed "Glc mitochondria," Fig. 2*A*) consume significantly less oxygen under such conditions.

Such physiological differences were accompanied by striking alterations in the subproteome of the respective mitochondrial membrane proteins (Fig. 2*B*, Supplemental Fig. 1, and Supplemental Table 1). We separated Glc and Lac membrane protein extracts by 2-DE and compared subsequent raw master gels using the Z3 software package (Fig. 2*B*). Although the limitations of 2-DE in separating highly hydrophobic proteins have been reported (49), the overlay of respective raw master gels clearly indicated significant differences between the two mitochondrial extracts (Fig. 2*B* and Supplemental Table 1). Subsequent analysis by mass spectrometry of proteins showing prominent alterations revealed a strong enrichment for D-lactate ferricytochrome *c* oxidoreductase 1 (DLD1) in Lac mitochondria (Table I and Supplemental Table 1, spot numbers 2–4). This finding agrees with a previous report showing induction of this protein in Lac and suppression in Glc mitochondria (50). We also observed alterations in the amounts of several other mitochondrial membrane proteins (Fig. 2*B*, Supplemental Table 1, and Supplemental Fig. 1B). Whereas enrichment of the outer membrane proteins OM45 and VDAC1 occurred, TOM70 was decreased in Lac compared with Glc mitochondria. These results were confirmed by protein analysis of isolated outer mitochondrial membranes and immunoblotting analysis of whole mitochondria (Fig. 6 and below). Similar regulation of OM45, VDAC1, and TOM70 upon Glc exhaustion and shift toward respiration has been reported at the transcriptome level (51). Moreover and in agreement with observed differences in respiratory capacity (Fig. 2*A*), proteins belonging to complexes of the respiratory chain (Table I and Supplemental Table 2) were present in significantly higher amounts in Lac than Glc mitochondria (Fig. 2*B*, Supplemental Fig. 1, and Supplemental Table 1). Due to their location within the mitochondrial inner membrane, which consists of ~75% protein by weight (52, 53), depletion of these proteins does not only alter the physiology of mitochondria but the structural properties of the organelle as well. Consequently and in contrast to Lac mitochondria, Glc mitochondria are highly sensitive structures with a tendency toward disruption upon handling.

Initially ZE-FFE analysis of Glc mitochondria resulted in very broad peaks (Fig. 2*C*, *left panel*) that could be attributed to morphological heterogeneity of the disrupted organelles (Fig. 2*C*, *right panel*). Substantial improvement of the separation profiles was obtained (Fig. 2*D*, *left panel*) by adjusting the ZE-FFE separation buffer to a slightly hyperosmotic sucrose concentration (0.5 *versus* 0.3 M) as well as minimizing shear forces during the isolation procedure. Consequently we ob-

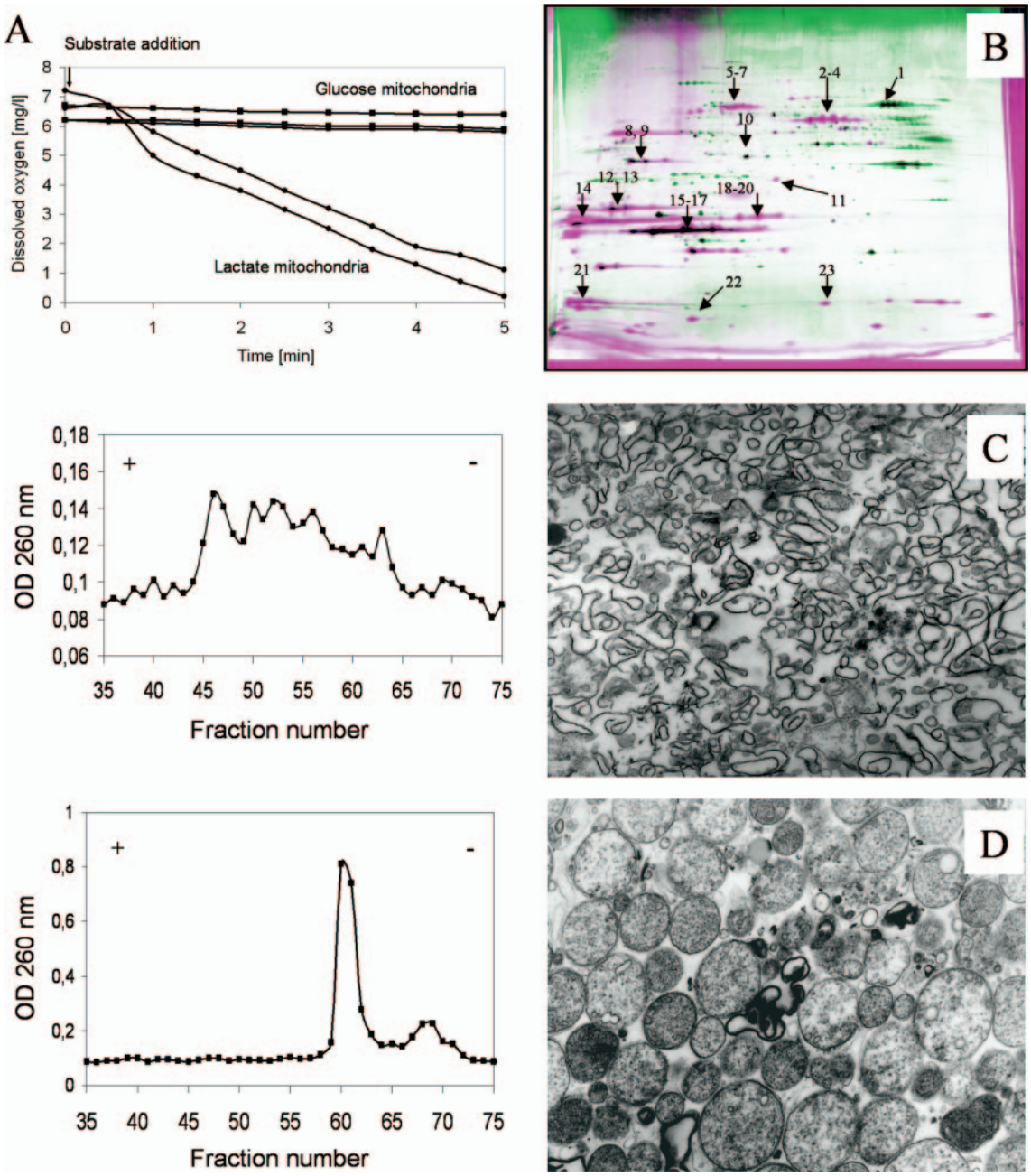

FIG. 2. **Glucose mitochondria differ from lactate mitochondria and can be analyzed by ZE-FFE only under optimized conditions.** *A*, mitochondria isolated from yeast grown in Glc media consume minimal oxygen in contrast to mitochondria isolated from cells grown in lactate that show strong respiratory activity (substrate, 1% ethanol); each graph represents an independent mitochondrial preparation. *B*, physiological differences between Glc and Lac mitochondria are reflected by a marked change in abundance of membrane proteins. Integral membrane proteins were enriched by sodium carbonate treatment, solubilized with dodecylmaltoside or Triton X-100, and resolved by 2-DE (sample load, 50 μg; IPG 3–10 non-linear, SDS-PAGE 9–14% T). Three representative gels were pooled to a raw master gel by Z3 software; Glc mitochondria membrane proteins are shown in *green*, and Lac mitochondria membrane proteins are shown in *magenta*. The overlay highlights the differences between the two conditions. *Arrows* indicate the identified proteins (Table I and Supplemental Table 2). For determination of protein spot intensities see Supplemental Fig. 1 and Supplemental Table 1). *C*, ZE-FFE separation profile (*left panel*) of a single Glc mitochondria preparation that has been subjected to considerable disruption (*right panel*; *magnification*, 32,000). Profiles showed broad peaks spanning many fractions with low signal to noise ratio (anode, +; cathode, −). *D*, ZE-FFE separation profile (*left panel*) of a single Glc mitochondria preparation containing mostly intact organelles (*right panel*; *magnification*, 32,000). Separation conditions were optimized compared with *C* (*i.e.* buffer temperature, osmolarity, flow velocity, and importantly avoidance of shear forces during preparation).

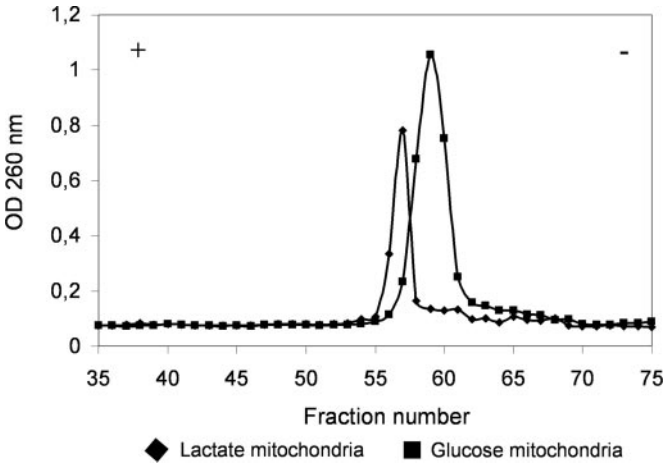

FIG. 3. **Glucose and lactate mitochondria differ in their electrophoretic behavior.** ZE-FFE analysis of Glc and Lac mitochondria demonstrated differences in deflection patterns: Lac mitochondria deflected two to three fractions further toward the anode (+) than Glc. Furthermore Lac mitochondria were found within a sharp ZE-FFE peak spanning two to three fractions, whereas Glc mitochondria were found in slightly broader peaks spanning four to five fractions.

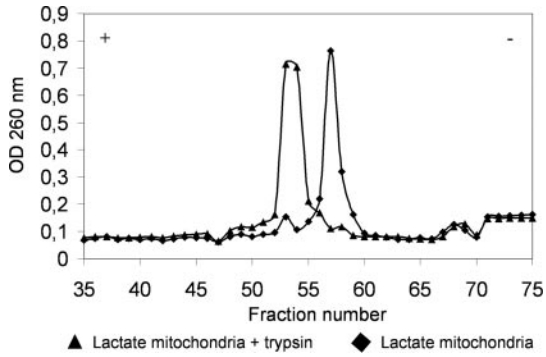

FIG. 4. **The deflection of mitochondria in the electric field depends on their surface proteome.** Mild surface proteolysis of Lac mitochondria with trypsin induced a shift of three to four fractions toward the anode compared with untreated controls (here from fraction 57 to fraction 53/54) (anode, +; cathode, −).

served a major peak spanning approximately three to four fractions containing a homogeneous mitochondrial population with intact membranes (Fig. 2*D*, *right panel*). This finding shows that, in addition to its use as a preparative tool for isolating mitochondria, ZE-FFE can also serve under well defined parameters as an analytical tool for discriminating ruptured and intact organelle preparations.

S. cerevisiae Mitochondria with Altered Respiratory Activity Show Different Deflection Properties in ZE-FFE—We compared Glc *versus* Lac mitochondria isolated from yeast in logarithmic growth phase to determine whether these organelle populations differed in their electrophoretic deflection. Whereas Lac mitochondria (Fig. 1*B*, *right panel*) were collected in very sharp peaks, usually about two fractions, Glc mitochondria were found in slightly broader peaks spanning three to four fractions (Fig. 2*D*, *left panel*). Moreover we found a different electrophoretic deflection of these two mitochondrial populations (Fig. 3) whereby Lac mitochondria deflected two to three fractions further toward the anode. This "anodal shift" was highly reproducible and observed consistently throughout all experiments irrespective of the ZE-FFE device used and the individual mitochondrial preparation under analysis. This method is therefore effective in detecting biological differences because no labeling or additional modifications were applied to the samples under analysis in these comparisons.

The Electrophoretic Deflection Properties of Different Mitochondria Can Be Modified by Means That Affect the Surface Proteome—A fundamental parameter proposed to be responsible for the degree of deflection in ZE-FFE is the surface charge (54). Yeast mitochondria and more precisely their outer membranes contain several negatively charged lipids

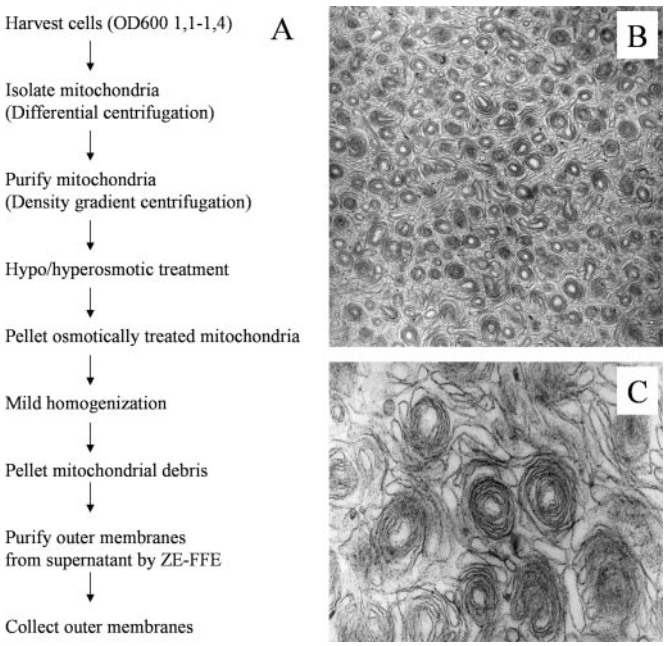

FIG. 5. **Isolation of outer mitochondrial membranes by ZE-FFE.** *A*, flow chart for outer mitochondrial membrane isolation procedure. *B* and *C*, electron micrographs of isolated Lac outer mitochondrial membranes (*magnification*, 16,000 and 80,000).

(*e.g.* phosphatidylinositol, phosphatidylserine, phosphatidylglycerol, and free acid (55)) as well as ~30 different protein species (MitoP2 database, release June 2004, ihg.gsf.de/mitop2/start.jsp). The charges contained herein protrude into the cytosol to various extents (56).

To estimate the degree to which these outer membrane proteins contribute to the observed ZE-FFE deflection, we exposed the organelles to a limited trypsin treatment. Mild proteolytic treatments have been reported to leave organelles intact but cleave off the cytosolic parts of the protruding proteins (24, 57, 58). In fact, deflection of mitochondria was altered upon trypsin treatment (Fig. 4). We could observe

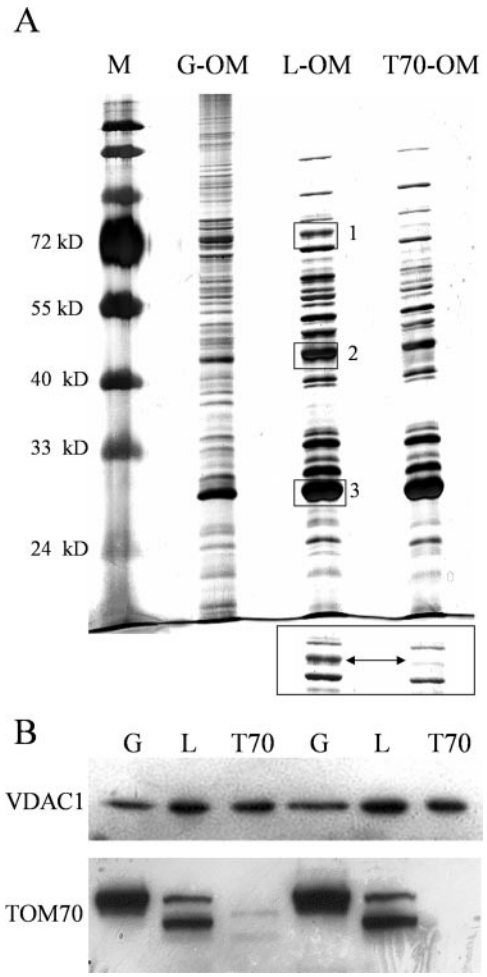

FIG. 6. **Different mitochondrial populations display varying protein composition of the outer mitochondrial membranes.** *A*, comparison of outer mitochondrial membrane protein extracts resolved by SDS-PAGE and visualized by silver stain. Outer mitochondrial membranes were isolated from Glc (*G-OM*), Lac (*L-OM*), and ΔTOM70 (*T70-OM*) mitochondria. *Numbered rectangles* define the outer mitochondrial membrane proteins TOM70 (*1*), OM45 (*2*), and VDAC1 (*3*). G-OM and L-OM protein patterns appeared to be markedly different. In contrast, L-OM and T70-OM protein patterns were highly similar except for the absence of an apparent TOM70 band in T70-OM (*magnified inset*). Protein load per lane, 2 μg; *M*, protein standard. *B*, immunoblotting analysis of protein extracts from isolated Glc (*G*), Lac (*L*), and ΔTOM70 (*T70*) mitochondria. *Upper panel*, Lac and ΔTOM70 mitochondria contain higher VDAC1 levels than Glc mitochondria. Protein load per lane, 10 μg. *Lower panel*, Glc mitochondria contain higher TOM70 levels than Lac mitochondria. The origin of the double band TOM70 signal in lactate mitochondria is currently unknown. TOM70 was not detected in ΔTOM70 mitochondria. Protein load per lane, 20 μg.

"anodal shifts" for both Lac (approximately three to four fractions, Fig. 4) and Glc mitochondria (two fractions, data not shown). Given the marked alteration in deflection of treated mitochondria, we conclude that the cytosol-oriented parts of outer mitochondrial proteins significantly contribute to the degree of deflection in ZE-FFE.

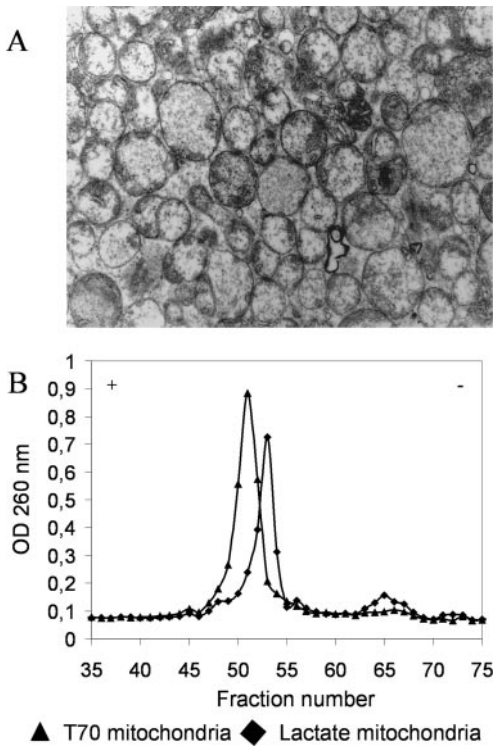

FIG. 7. **Deletion of a single protein species in the mitochondrial outer membrane alters ZE-FFE migration of whole organelles.** *A*, electron micrograph of ΔTOM70 mitochondria (*magnification*, 32,000). *B*, ZE-FFE separation profiles for ΔTOM70 (*T70*) and Lac mitochondria demonstrating main peaks of comparable shape for both populations. However, an anodal shift of one to two fractions was observed in ΔTOM70 mitochondria compared with Lac mitochondria.

Mitochondrial Populations with Different ZE-FFE Deflection Also Vary in the Protein Composition of Their Outer Membranes—Because we observed a strong alteration in deflection for Lac mitochondria upon proteolytic treatment but a weaker effect on Glc mitochondria, we investigated the extent to which these organelles differed in their surface proteomes. Outer mitochondrial membranes were isolated (Fig. 5, *A* and *B*), and protein composition was analyzed by SDS-PAGE. Three prominent bands (Fig. 6*A*) were identified as TOM70, OM45, and VDAC1, respectively (Table II and Supplemental Fig. 2), confirming the identity of the isolated structures (56). Fig. 6*A* shows that Glc and Lac outer mitochondrial membranes (*G-OM versus L-OM*) differed in the amount of these three proteins. In contrast to Lac mitochondria, Glc mitochondria contained lesser amounts of the major outer mitochondrial membrane proteins VDAC1 and OM45 (see also Fig. 2*B*) and only slightly higher of TOM70 protein (Fig. 6, *A* and *B*). This finding may explain the underlying reason for the observed increased effect of proteolytic treatment on Lac mitochondria.

Deleting a Single (Major) Protein Species in the Mitochondrial Outer Membrane Alters the ZE-FFE Migration of the Organelle—To further investigate the effect of outer mito-

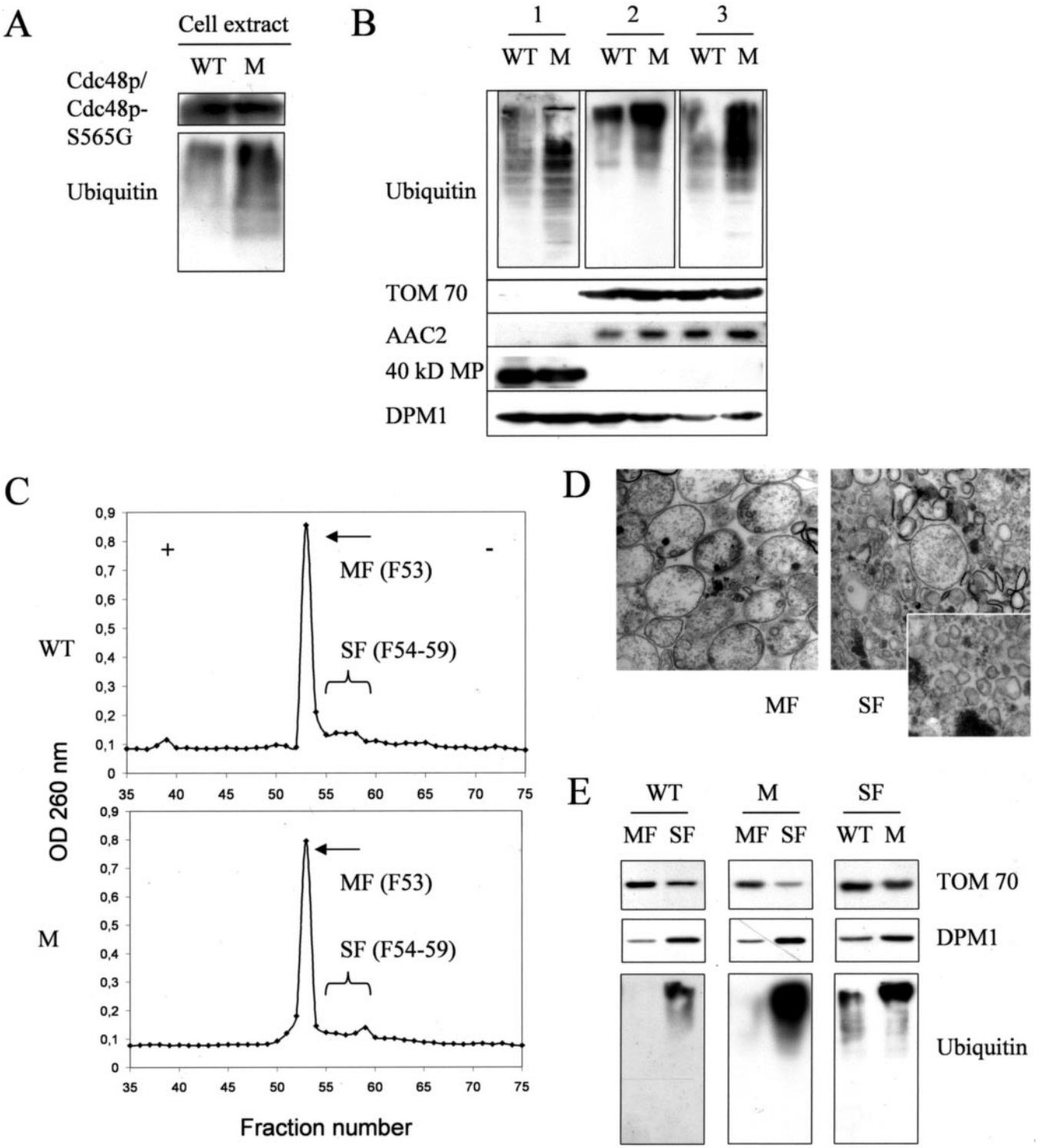

FIG. 8. **Isolation of a mitochondrial side fraction by ZE-FFE from an apoptotic yeast mutant showing strong polyubiquitination and association with microsomes.** *A*, immunoblotting analysis of whole cell extracts from galactose-grown yeast cultures expressing wild-type Cdc48p (*WT*) or mutant Cdc48p-S565G (*M*). Polyubiquitinated proteins accumulate in the *cdc48*^{S565G} strain. Protein load per lane was 15 μg. *B*, subcellular fractions of wild-type (*WT*) and *cdc48*^{S565G} mutant strains (*M*) under apoptotic conditions. *Column 1*, in the mutant strain polyubiquitinated proteins accumulate in microsomes; *column 2*, mitochondria isolated by differential centrifugation; *column 3*, gradient-purified mitochondria. TOM70 (outer mitochondrial membrane) and AAC2 (inner mitochondrial membrane) were used as validation for mitochondria; 40-kDa microsomal protein and DPM1 were used as validation for light and heavy microsomes, respectively. Protein load per lane was 10 μg. *C*, ZE-FFE separation profiles of mitochondrial preparations isolated from wild-type (*WT*) and *cdc48*^{S565G} (*M*) strains under

chondrial proteins on ZE-FFE deflection properties and because Lac and Glc mitochondria also differ in several other aspects, such as their lipid composition (59), we sought a more stringent comparison of mitochondrial populations. Thus we isolated mitochondria from a TOM70 deletion mutant (Fig. 7*A*) as TOM70 is a high molecular weight protein (617 amino acids) residing in the mitochondrial outer membrane with its major aspect directed toward the cytosol carrying a surplus of negative charges. Consequently its absence/presence in the outer mitochondrial membrane would be expected to result in a differential electrophoretic behavior.

Whereas TOM70 could be detected and subsequently identified by mass spectrometry from outer mitochondrial membranes of wild-type Lac mitochondria (*L-OM*), no apparent protein band was observed in respective samples of ΔTOM70 Lac mitochondria (*T70-OM*; Fig. 6*A*, *magnified inset*). Immunoblotting analysis of whole mitochondria confirmed the deletion of TOM70 in ΔTOM70 Lac mitochondria (Fig. 6*B*, *lower panels*). In contrast, VDAC1 was detected in comparable amounts in both wild-type and ΔTOM70 mitochondria (Fig. 6*B*, *upper panels*). Despite the lack of TOM70, however, the protein patterns of isolated outer mitochondrial membranes from wild-type and ΔTOM70 mitochondria isolated from yeast strains grown in Lac media appeared highly similar (Fig. 6*A*, *L-OM versus T70-OM*). Thus, analysis of the major abundant proteins indicated that wild-type mitochondria and ΔTOM70 mitochondria differ in one protein species in their outer membranes, TOM70.

Subsequent analysis by ZE-FFE confirmed the differentiating properties of this technique. Whereas separation profiles for both populations resulted in main peaks of comparable shape and spanning two to three fractions, they differed, however, in their deflection (Fig. 7*B*): ΔTOM70 mitochondria shifted one to two fractions further toward the anode than wild-type mitochondria (Fig. 7*B*), enabling us to discriminate between these organelles. Furthermore both mitochondrial populations displayed anodal shifts upon proteolytic shedding of cytosolic parts of the outer mitochondrial surfaces (data not shown). Interestingly wild-type and ΔTOM70 mitochondria were collected in similar fractions upon protease treatment. Because the two surface proteomes significantly differed only in the presence/absence of TOM70 and because surface proteolysis abolishes this altered behavior, the difference observed in ZE-FFE deflection may be attributed to the presence/absence of a single protein species, TOM70.

Accumulation of Polyubiquitinated Proteins in Mitochondria Isolated from an Apoptotic Yeast Strain—The above examples demonstrate that ZE-FFE can be successfully applied to distinguish between different mitochondrial populations from yeast. Consequently we directed our attention toward the comparison of yeast mitochondria isolated from pathophysiological cellular backgrounds.

The mutant variant Cdc48p-S565G of the essential protein Cdc48p was the first apoptotic regulator found in bakers' yeast (16). Fundamental cellular processes, such as the ubiquitin-dependent ER-associated protein degradation pathway (ERAD), have been linked to Cdc48p (18, 19). Consistently we observed accumulation of polyubiquitinated proteins in whole cell extracts (Fig. 8*A*) and especially in microsomal fractions (Fig. 8*B*, *column 1*) of the *cdc48*^{S565G} strain but less polyubiquitination in the wild-type strain (Fig. 8, *A* and *B*).

Interestingly we also observed a strong accumulation of polyubiquitinated proteins in mitochondrial fractions (Fig. 8*B*, *column 2*), suggesting that cellular stress imposed by ERAD dysfunction upon *CDC48* mutation is conferred to mitochondria. In fact, upon further purification of mitochondria by sucrose gradient centrifugation, we still observed polyubiquitination in gradient-purified mitochondrial samples (Fig. 8*B*, *column 3*). Light microsomes, as evidenced by the 40-kDa microsomal marker protein, were completely depleted from mitochondrial samples (Fig. 8*B*). However, detectable amounts of heavy microsomes, especially in the *cdc48*^{S565G} strain as evidenced by the presence of dolichol-phosphate mannosyltransferase (DPM1), remained associated with mitochondria (Fig. 8*B*). Due to the failure to avoid this stable co-purification by "classical" preparation methods, especially in the *cdc48*^{S565G} strain, we reasoned that mitochondria strongly associated with microsomes should deflect differently in the electric field compared with non-associated "pure" mitochondria and therefore subjected the mitochondrial preparations to ZE-FFE.

A Mitochondrial Side Fraction Showing Strong Polyubiquitination Signals and Association with Microsomes Can Be Isolated by ZE-FFE—The ZE-FFE separation profiles of mitochondrial samples of both wild-type and mutant displayed a main peak with equal deflection (Fig. 8*C*, fraction 53 (*F53*) in the displayed example). EM analysis characterized these main fractions (*MF*) as containing intact mitochondria with a high degree of purity (Fig. 8*D*, exemplarily shown for the mutant main fraction), and hardly any other organelles were observed in these fractions. In addition, side fractions (*SF*, fractions 54–59 (*F54–59*)) were obtained by ZE-FFE in both wild-type

apoptotic conditions showing main (*MF*) and side (*SF*) fractions for each strain. *F*, fraction. *D*, electron micrograph of the main fraction (*MF*, *left*) and side fraction (*SF*, *right*) of the *cdc48*^{S565G} strain under apoptotic conditions. Besides mitochondria, the side fraction of this strain contains mitoplasts, high contrast membranous structures, and low contrast microsomal vesicles (*magnified panel*). *E*, characterization of ZE-FFE fraction by immunoblotting analysis. ZE-FFE main (*MF*) and side fraction (*SF*) extracts for both wild-type (*WT*) and mutant (*M*) strains were analyzed under apoptotic conditions. TOM70 was used as validation for mitochondria, and DPM1 was used as validation for (heavy) microsomes. Fractions were further tested for polyubiquitination. No polyubiquitination was observed in the main fractions, but very strong polyubiquitination was detected in the side fraction of the mutant. Protein load per lane was 10 μg.

and mutant strain (Fig. 8*C*). In contrast to the main fractions, characterization of the side fractions by EM revealed an inhomogeneous content. In addition to mitochondria, a higher portion of membranous structures, mitoplasts, and microsomal vesicles were observed especially in mitochondrial samples from the *cdc48*^{S565G} strain (Fig. 8*D*). Immunoblotting analysis confirmed the enrichment of microsomal content compared with the respective main fractions (DPM1, Fig. 8*E*) but also demonstrated the presence of mitochondria (TOM70, Fig. 8*E*) in these ZE-FFE side fractions. Thus, using ZE-FFE we were able to enrich non-associated pure mitochondria (main fractions) from mitochondria associated with microsomes (side fractions). Importantly hardly any polyubiquitination was detected in the main fractions of both wild-type and *cdc48*^{S565G} strains (Fig. 8*E*). In contrast, comparing the mitochondrial side fractions, we found very strong polyubiquitination signals in the mutant strain (Fig. 8*E*). Thus, in the *cdc48*^{S565G} strain a stable co-purification of microsomes with only a subset of mitochondria coincides with abnormally increased polyubiquitination, the cellular damage/stress marker associated with this apoptotic yeast strain.

DISCUSSION

This study shows that ZE-FFE is an effective analytical sensor able to demonstrate diversities in mitochondrial populations isolated from yeast that can be linked to discrete physiological or molecular determinants inherent to specific mitochondria variants. Importantly these biological differences were discriminated by ZE-FFE in an unbiased fashion as no labeling or additional modifications were applied to these mitochondria under study.

With the experimental specifications given under "Experimental Procedures" we obtained ZE-FFE separation profiles of mitochondria spanning only a few fractions. Given this high resolution for a specific mitochondrial sample, we then aimed at comparing various mitochondrial populations and termed this approach ZE-FFE in analytical mode. An additional advantage of this approach was the highly purified resultant mitochondrial population evidenced by electron micrograph inspection of mitochondrial samples (*e.g.* Figs. 1*B* and 2*D*).

ZE-FFE in Analytical Mode Enables Quality Assessment of Mitochondrial Preparations and Analysis of Different Mitochondrial Populations—We were able to show that ZE-FFE in analytical mode enables the differential analysis of mitochondrial populations as follows.

(i) Markedly different separation profiles for Lac mitochondria purified with or without additional sucrose density gradient centrifugation were obtained (Fig. 1, *cf. A* and *B*, *right panels*). Because the inner mitochondrial membrane is sucrose-impermeable, mitochondria purified by sucrose gradients are exposed to hyperosmotic conditions, resulting in heterogeneity of shape and degree of matrix condensation as can be seen on electron micrographs (Fig. 1*A*, *left panel*). Remarkably this heterogeneity occurred despite iso-osmotic incubation and separation conditions prior to and following the density gradient and moreover was detectable by ZE-FFE. In contrast, mitochondria isolated by differential centrifugation were homogeneous and characterized by sharp peaks (Fig. 1*B*, *left panel*). This finding may be explained by a certain degree of irreversible alterations in some mitochondria induced by sucrose density gradient centrifugation, resulting in a limited ability of affected mitochondria to readjust both shape and degree of matrix condensation in response to subsequent experimental iso-osmotic conditions. Consequently this heterogeneity in mitochondrial appearance could result in altered electrophoretic deflection.

(ii) We analyzed a Glc mitochondria preparation damaged by shearing forces. One important reason for their structural sensitivity may be the low expression levels of several inner membrane proteins, including those of respiratory complexes (Fig. 2*B*). When damaged by vigorous handling, these mitochondria separate into broad peaks with low signal to noise ratio spanning over 10 fractions (Fig. 2*C*). In contrast, preparations containing mostly intact organelles typically present with one major peak having high signal to noise ratio and spanning only four fractions (Fig. 2*D*). Thus, ZE-FFE not only allows isolation of mitochondria in high purity but also enables an estimation of the overall integrity of the isolated mitochondria and thus the quality of a given mitochondrial preparation.

(iii) Comparison of intact Glc and Lac mitochondria by ZE-FFE in analytical mode revealed differential deflections of both populations (Fig. 3). Thus, ZE-FFE is sensitive to the biological differences of these two populations (Fig. 2, *A* and *B*; below).

The Electrophoretic Deflection of Different Mitochondria Is Dependent on Organelle Charge, Hydrodynamic Properties, and Surface Proteome—Which parameters determine particle deflection, and why do Glc and Lac mitochondria deflect differently in an electric field?

We found that both organelle populations deflected toward the anode, confirming earlier reports (29, 60) that they are overall negatively charged at a neutral pH. Thus, surface charge is a fundamental parameter influencing the deflection behavior of the organelles.

Another question of interest was why do Lac and Glc mitochondria deflect differently in ZE-FFE? The estimated average particle diameter of ZE-FFE-purified Glc and Lac mitochondria obtained by electron microscopy were of comparable sizes (0.76 *versus* 0.72 μm, respectively). As can be seen on the electron micrographs, however, both populations comprise mitochondria with varying diameters, which can evidently be explained by variation of the section plane (50-nm slice) obtained by the ultramicrotome but hampers a clear conclusion on the importance of the mitochondrial size on their respective deflection. Another difficulty is to assess whether and to which extent aggregated mitochondria travel through the separation chamber (28). An advantage of the ZE-FFE technique is, however, that aggregated mitochondrial clumps are, if they occur, clearly visible in the separation

chamber and that conditions that favor aggregation of mitochondria were carefully avoided/minimized during their analysis (see "Experimental Procedures"). Thus, although it cannot be excluded that smaller not visible mitochondrial aggregates have formed, it seems unlikely that the reproducibly observed ZE-FFE separation profiles and differences in deflection are primarily due to a rather unspecific aggregation. However, Glc mitochondria appeared more deformable than Lac mitochondria and were highly sensitive toward disruption (Fig. 2, *C* and *D*). This structural difference may result in higher flow resistance of Glc *versus* Lac mitochondria and could explain a slower deflection toward the anode. Consequently varying deflection velocities in the electric field would not only depend on the charge of the organelle but also on its hydrodynamic properties.

Our results of the tryptic surface proteolysis treatments of mitochondria strongly support this conclusion. Glc mitochondria outer membranes contain three major abundant proteins (Fig. 6*A*): VDAC1, OM45, and TOM70. Adams *et al.* (24) have convincingly shown that trypsin treatment of outer mitochondrial membranes cleaves off the cytosolic parts of such outer membrane proteins as TOM70. In contrast, proteins that are more embedded within the outer membrane (*e.g.* VDAC1) remain unaffected by proteolysis (24). As a result, the abundant outer mitochondrial membrane proteins OM45 and TOM70 are primarily affected by this treatment because these proteins protrude into the cytosol (amino acids 23–393 for OM45 and 31–617 for TOM70, Swiss-Prot entries, respectively). In the case of OM45, the cytosolic protein portion contains rather balanced positive and negative charges (73 positive *versus* 71 negative charges, Swiss-Prot ProtParam tool), but there is an overhang of negative charges for TOM70 (85 positive *versus* 101 negative charges). Assuming cleavage between amino acids 23–32 and 38–50 for OM45 and TOM70, respectively, a net removal of negative charges would occur. Consequently mitochondria whose surface is more positive charged following protease treatment, compared with untreated mitochondria, should deflect more to the negative pole (cathode) in ZE-FFE. Our results show, however, that the opposite is true (Fig. 4) whereby protease-treated mitochondria deflected more to the positive pole (anode). It seems therefore likely that removal of cytosolic protein domains smoothed the outer mitochondrial surface thereby altering the hydrodynamic properties of the organelles and causing a faster deflection of treated mitochondria toward the anode, thus outweighing the altered surface charge.

In support of this notion are results of experiments that were aimed at the removal of cytosol-oriented protein-dependent positive surface charges on electrophoretic deflection (data not shown). Thereto mitochondria were incubated with *N*-hydroxysulfosuccinimidyl acetate to acetylate lysine residues of mitochondrial outer membrane proteins. Such a treatment should yield mitochondria that are more negatively charged and thus deflect more to the positive pole (anode). In fact, treated rat liver mitochondria markedly deflected toward the anode (data not shown). Using such experimental conditions with yeast mitochondria, however, we observed either a lack of shift or, in some cases, unexpectedly a slight shift (one fraction) toward the negative pole (cathode) (data not shown). These results support the notion of a minor importance of cytosol-oriented protein-dependent charges in the fine tuning of ZE-FFE deflection of yeast mitochondria. However, future studies have to further substantiate these experiments, *e.g.* to quantitatively assess acetylation at the protein level and to investigate why ZE-FFE deflection of rat liver mitochondria was affected by such treatments whereas deflection of yeast mitochondria was not.

From these data, two important conclusions can be drawn. (i) Given significant differences, the surface proteome determines mitochondrial structural subtleties that may be detected by ZE-FFE in analytical mode because Glc and Lac mitochondria differ in their surface proteomes and display altered electrophoretic deflection. (ii) Under ZE-FFE in analytical mode, the hydrodynamic differences of yeast mitochondria may add to/superimpose the differences in charge of their respective surface proteomes because membrane smoothing induced pronounced changes in electrophoretic deflection whereas blocking of surface charges did not.

These conclusions can be challenged experimentally: we compared wild-type *S. cerevisiae* mitochondria with mitochondria showing a deletion in the high molecular weight outer membrane protein TOM70 whose major segment protrudes into the cytosol (56) carrying a surplus of negative charges. Regarding their surface proteome, ΔTOM70 mitochondria lack two features in comparison with its wild-type counterpart: a high molecular weight protein species and several negative charges. The first feature could lead to mitochondria with altered surface that would show a higher electrophoretic deflection velocity (toward the anode), whereas the second feature could lead to a shift toward the cathode.

Indeed we observed an anodal shift of one to two fractions of ΔTOM70 mitochondria compared with wild-type mitochondria (Fig. 7*B*), supporting the hypothesis about altered surface properties influencing the deflection behavior. The observed anodal shift for ΔTOM70 mitochondria strongly argues against protein-dependent charge as the sole determinant for deflection. Nevertheless the altered ΔTOM70 surface proteome compared with wild-type mitochondria is sufficient to cause different electrophoretic deflection of the whole organelle.

Analysis of a Pathologically Altered Mitochondrial Subpopulation with ZE-FFE in Analytical Mode—To further assess the benefits of ZE-FFE in analytical mode, we directed our interest toward the comparison of yeast mitochondria isolated from different pathophysiological cellular backgrounds.

The mutant protein Cdc48p-S565G was the first apoptotic regulator found in bakers' yeast (16) that leads to a charac-

teristic apoptotic cellular phenotype: phosphatidylserine externalization, DNA fragmentation, chromatin condensation and nuclear fragmentation, vacuolization, and ER expansion (16, 22). A key element of wild-type Cdc48p is its role in the ubiquitin-dependent ERAD (61–63). Screening different *cdc48* mutants for ERAD activity revealed that the efficiency of this protein degradation pathway is decreased in the *cdc48*^{S565G} strain compared with the wild-type strain (17). Consistently we observed accumulation of polyubiquitinated proteins (Fig. 8*A*) in whole cell extracts of the *cdc48*^{S565G} strain. Subsequent analysis of subcellular compartments localized accumulating polyubiquitinated proteins to microsomal and mitochondrial extracts (Fig. 8*B*). Moreover in the *cdc48*^{S565G} strain, polyubiquitination as well as significant amounts of (heavy) microsomes remained stably associated with mitochondria upon sucrose gradient centrifugation (Fig. 8*B*).

Because the above results showed that hydrodynamic effects, among others, influence the deflection of yeast mitochondria in ZE-FFE, we reasoned that mitochondria strongly associated with microsomes should deflect differently in the electric field when compared with non-associated pure mitochondria. Indeed by applying ZE-FFE, we were able to separate a mitochondrial main population enriched with non-associated mitochondria (main fractions) from mitochondria associated with microsomes (side fractions) (Fig. 8, *C*, *D*, and *E*). This analysis revealed that (i) the majority of the mitochondria (*i.e.* the main fraction) from the *cdc48*^{S565G} strain show a high degree of intactness and no altered electrophoretic deflection compared with wild-type mitochondria, (ii) the majority of the mitochondria (*i.e.* the main fraction) collected after ZE-FFE from the *cdc48*^{S565G} strain shows no polyubiquitination, and most importantly (iii) a subset of the mitochondria (*i.e.* the side fraction) from the *cdc48*^{S565G} strain, isolated by ZE-FFE, show stable co-purification with microsomes and very strong polyubiquitination signals.

Thus, the majority of mitochondria seems to be unaffected by polyubiquitination upon *CDC48* mutation, although classical isolation methods (*i.e.* differential and gradient centrifugation) suggested otherwise. ZE-FFE could thus demonstrate that only a subset of mitochondria is involved in such pathological subcellular alterations in the *cdc48*^{S565G} strain.

A possible explanation for the deleterious link between a mitochondrial subpopulation and the ER in the *cdc48*^{S565G} strain might be the following. Upon *CDC48* mutation (*cdc48*^{S565G}), an enrichment of polyubiquitinated proteins at the ER demonstrates the malfunction of the ERAD pathway, leading to ER expansion, as was observed in earlier studies (16). These deleterious processes could be transferred to some mitochondria through the aggregation of the affected ER structures with mitochondrial membranes. This would explain the significantly higher amount of polyubiquitination and microsomes co-purifying with a subset of mitochondria in this mutant strain. Clearly future studies have to further substantiate this hypothesis. It is interesting, however, that we observed a quantitatively increased spatial proximity between these two organelles in the *cdc48*^{S565G} strain compared with wild-type using an ultrastructural analysis by electron microscopy (data not shown).

ZE-FFE Is an Additional and Complementary Technique for the Analysis of Mitochondrial Heterogeneity—In addition to a decisive role in apoptosis, structural and molecular alterations in mitochondria appear to be critical factors in the pathology of many diseases. To analyze these alterations at the molecular level and clarify the reasons why some organelles appear more affected and vulnerable than others, analytical and preparative tools able to resolve this heterogeneity are indispensable.

A whole plethora of analytical techniques has been applied for the subcellular analysis of mitochondria (5). Thereto density gradient-purified mitochondria have been widely used for most experimental approaches (5), which, however, did analyze the overall/averaged properties of mitochondria and did hardly assess their potential heterogeneity. In a recent study, two mitochondrial subfractions differing in their buoyant densities were obtained by continuous flow ultracentrifugation (64). This study shows that mitochondrial subtypes may be separated given sufficient density-based heterogeneity of the starting sample. As an alternative approach, electrophoretic methods relying on a different separation parameter, *i.e.* the electrophoretic mobility, have been applied, such as high resolution density gradient electrophoresis (65, 66) or capillary electrophoresis (CE). Especially CE has been applied in more recent studies for the analysis of individual mitochondria (67), for the estimation of the cardiolipin content of single mitochondria (28), to monitor effects of cellular disruption techniques on single mitochondrial mobility (68), and to analyze individual mitochondria directly sampled from tissue cross-sections (69). Evidently from these exciting studies, electrophoretic methods are a very promising approach to study mitochondrial heterogeneity. Our present results show that ZE-FFE, as analytical sensor, may also contribute significantly in this respect. Besides the advantage of being a preparative method yielding sufficient organelles for further analyses like proteomics (in comparison to CE), we report here the further subfractionation of a mitochondrial preparation considered to be homogeneous according to the state of the art. It will be interesting to see whether this approach will also open the door to a detailed analysis of other pathological states where mitochondria are involved.

We would like to emphasize the fact that our study was conducted on mitochondria isolated from yeast. Although mitochondria isolated from mammalian sources reveal high similarities to the yeast counterpart, there are also significant differences: mouse liver mitochondria isolated by sucrose gradient centrifugation displayed marked tailing effects (data not shown) comparable to the profile shown in Fig. 1*A*. Our attempts to alter the surface charge by blocking amino

groups, however, had a significant effect on the deflection of rat liver mitochondria in contrast to the yeast mitochondria that showed no effect upon treatment. Therefore it appears that mitochondria from mammalian sources display a higher charge density on their outer membranes and that charges carried by proteins are of much stronger importance for their electrophoretic deflection. These differences are currently under investigation and should be considered in the analysis of mitochondria from higher animals.

Acknowledgments—We thank S. Willmann and A. Brandt for excellent technical assistance and express thanks to Drs. E. E. Rojo and U. Olazabal for critical reading of the manuscript. We also thank Dr. A. Borst for support with electron microscopy and Drs. W. Neupert and G. Daum for the kind gift of diverse antibodies.

* This work was supported by the German Federal Ministry for Education and Research (BMBF) Grants FKZ:031U108A (Subproject B2), FKZ:031U108E (Subproject B3), and FKZ:01GR0449 (Subproject 9, NGFN2 SMP Proteomics) as well as by European Union Grant LSHG-CT-2003-505520 (INTERACTION PROTEOME). The costs of publication of this article were defrayed in part by the payment of page charges. This article must therefore be hereby marked "*advertisement*" in accordance with 18 U.S.C. Section 1734 solely to indicate this fact.

S The on-line version of this article (available at http://www.mcponline.org) contains supplemental material.

¶ To whom correspondence should be addressed: Inst. of Toxicology, GSF-National Research Center for Environment and Health, Ingolstaedter Landstrasse 1, 85764 Munich-Neuherberg, Germany. Tel.: 49-89-3187-2663; Fax: 49-89-3187-3449; E-mail: zischka@gsf.de.

REFERENCES

1. Frank, S., Robert, E. G., and Youle, R. J. (2003) Scission, spores, and apoptosis: a proposal for the evolutionary origin of mitochondria in cell death induction. *Biochem. Biophys. Res. Commun.* **304,** 481–486
2. Bernardi, P., Scorrano, L., Colonna, R., Petronilli, V., and Di Lisa, F. (1999) Mitochondria and cell death. Mechanistic and methodological issues. *Eur. J. Biochem.* **264,** 687–701
3. Barja, G. (2004) Free radicals and aging. *Trends Neurosci.* **27,** 595–600
4. Fuller, K. M. and Arriaga, E. A. (2003) Advances in the analysis of single mitochondria. *Curr. Opin. Biotechnol.* **14,** 35–41
5. Olson, K. J., Ahmadzadeh, H., and Arriaga, E. A. (2005) Within the cell: analytical techniques for subcellular analysis. *Anal. Bioanal. Chem.* **382,** 906–917
6. Hsu, L. J., Sagara, Y., Arroyo, A., Rockenstein, E., Sisk, A., Mallory, M., Wong, J., Takenouchi, T., Hashimoto, M., and Masliah, E. (2000) α-Synuclein promotes mitochondrial deficit and oxidative stress. *Am. J. Pathol.* **157,** 401–410
7. Emerit, J., Edeas, M., and Bricaire, F. (2004) Neurodegenerative diseases and oxidative stress. *Biomed. Pharmacother.* **58,** 39–46
8. Reichert, A. S., and Neupert, W. (2004) Mitochondriomics or what makes us breathe. *Trends Genet.* **20,** 555–562
9. Taylor, S. W., Fahy, E., Zhang, B., Glenn, G. M., Warnock, D. E., Wiley, S., Murphy, A. N., Gaucher, S. P., Capaldi, R. A., Gibson, B. W., and Ghosh, S. S. (2003) Characterization of the human heart mitochondrial proteome. *Nat. Biotechnol.* **21,** 281–286
10. Mootha, V. K., Bunkenborg, J., Olsen, J. V., Hjerrild, M., Wisniewski, J. R., Stahl, E., Bolouri, M. S., Ray, H. N., Sihag, S., Kamal, M., Patterson, N., Lander, E. S., and Mann, M. (2003) Integrated analysis of protein composition, tissue diversity, and gene regulation in mouse mitochondria. *Cell* **115,** 629–640
11. Heazlewood, J. L., Tonti-Filippini, J. S., Gout, A. M., Day, D. A., Whelan, J., and Millar, A. H. (2004) Experimental analysis of the Arabidopsis mitochondrial proteome highlights signaling and regulatory components, provides assessment of targeting prediction programs, and indicates plant-specific mitochondrial proteins. *Plant Cell* **16,** 241–256
12. Sickmann, A., Reinders, J., Wagner, Y., Joppich, C., Zahedi, R., Meyer, H. E., Schonfisch, B., Perschil, I., Chacinska, A., Guiard, B., Rehling, P., Pfanner, N., and Meisinger, C. (2003) The proteome of Saccharomyces cerevisiae mitochondria. *Proc. Natl. Acad. Sci. U. S. A.* **100,** 13207–13212
13. Zischka, H., Weber, G., Weber, P. J., Posch, A., Braun, R. J., Büringer, D., Schneider, U., Nissum, M., Meitinger, T., Ueffing, M., and Eckerskorn, C. (2003) Improved proteome analysis of Saccharomyces cerevisiae mitochondria by free-flow electrophoresis. *Proteomics* **3,** 906–916
14. Prokisch, H., Scharfe, C., Camp, D. G., II, Xiao, W., David, L., Andreoli, C., Monroe, M. E., Moore, R. J., Gritsenko, M. A., Kozany, C., Hixson, K. K., Mottaz, H. M., Zischka, H., Ueffing, M., Herman, Z. S., Davis, R. W., Meitinger, T., Oefner, P. J., Smith, R. D., and Steinmetz, L. M. (2004) Integrative analysis of the mitochondrial proteome in yeast. *PLoS Biol.* **2,** 795–804
15. Hannig, K., and Wrba, H. (1964) Isolation of vital tumor cells by carrier-free electrophoresis. *Z. Naturforsch. B* **19,** 860
16. Madeo, F., Frohlich, E., and Frohlich, K. U. (1997) A yeast mutant showing diagnostic markers of early and late apoptosis. *J. Cell Biol.* **139,** 729–734
17. Jarosch, E., Taxis, C., Volkwein, C., Bordallo, J., Finley, D., Wolf, D. H., and Sommer, T. (2002) Protein dislocation from the ER requires polyubiquitination and the AAA-ATPase Cdc48. *Nat. Cell Biol.* **4,** 134–139
18. Wang, Q., Song, C., and Li, C. C. (2004) Molecular perspectives on p97-VCP: progress in understanding its structure and diverse biological functions. *J. Struct. Biol*. **146,** 44–57
19. Woodman, P. G. (2003) p97, a protein coping with multiple identities. *J. Cell Sci.* **116,** 4283–4290
20. Herrmann, J. M., Fölsch, H., Neupert, W., and Stuart, R. A. (1994) Isolation of yeast mitochondria and study of mitochondrial protein translation, in *Cell Biology: A Laboratory Handbook* (Celis, D. E., ed) pp. 538–544, Academic Press, San Diego, CA
21. Madeo, F., Schlauer, J., and Frohlich, K. U. (1997) Identification of the regions of porcine VCP preventing its function in Saccharomyces cerevisiae. *Gene* (*Amst.*) **204,** 145–151
22. Madeo, F., Fröhlich, E., Ligr, M., Grey, M., Sigrist, S. J., Wolf, D. H., and Fröhlich, K. U. (1999) Oxygen stress: a regulator of apoptosis in yeast. *J. Cell Biol.* **145,** 757–767
23. Fitton, V., Rigoulet, M., Ouhabi, R., and Guerin, B. (1994) Mechanistic stoichiometry of yeast mitochondrial oxidative phosphorylation. *Biochemistry* **33,** 9692–9698
24. Adams, V., Bosch, W., Schlegel, J., Wallimann, T., and Brdiczka, D. (1989) Further characterization of contact sites from mitochondria of different tissues: topology of peripheral kinases. *Biochim. Biophys. Acta* **981,** 213–225
25. Hannig, K. (1982) New aspects in preparative and analytical continuous free-flow cell electrophoresis. *Electrophoresis* **3,** 235–243
26. Krivankova, L., and Bocek, P. (1998) Continuous free-flow electrophoresis. *Electrophoresis* **19,** 1064–1074
27. Stahn, R., Maier, K. P., and Hannig, K. (1970) A new method for the preparation of rat liver lysosomes. Separation of cell organelles of rat liver by carrier-free continuous electrophoresis. *J. Cell Biol.* **46,** 576–591
28. Fuller, K. M., Duffy, C. F., and Arriaga, E. A. (2002) Determination of the cardiolipin content of individual mitochondria by capillary electrophoresis with laser-induced fluorescence detection. *Electrophoresis* **23,** 1571–1576
29. Heidrich, H. G., Stahn, R., and Hannig, K. (1970) The surface charge of rat liver mitochondria and their membranes. Clarification of some controversies concerning mitochondrial structure. *J. Cell Biol.* **46,** 137–150
30. Mayer, A. (1994) Inclusion of proteins into isolated mitochondrial outer membrane vesicles, in *Cell Biology: A Laboratory Handbook* (Celis, D. E., ed) pp. 545–549, Academic Press, San Diego, CA
31. de Kroon, A. I., Koorengevel, M. C., Goerdayal, S. S., Mulders, P. C., Janssen, M. J., and de Kruijff, B. (1999) Isolation and characterization of highly purified mitochondrial outer membranes of the yeast Saccharomyces cerevisiae (method). *Mol. Membr. Biol.* **16,** 205–211
32. Diekert, K., de Kroon, A. I., Kispal, G., and Lill, R. (2001) Isolation and subfractionation of mitochondria from the yeast Saccharomyces cerevisiae. *Methods Cell Biol.* **65,** 37–51
33. Rickwood, D., Dujon, B., and Darley-Usamar, V. M. (1988) Isolation of

mitochondria, in *Yeast—A Practical Approach* (Campbell, I., and Duffus, J. H., eds) pp. 219–222, IRL Press, Oxford
34. Meisinger, C., Sommer, T., and Pfanner, N. (2000) Purification of Saccharomyces cerevisiae mitochondria devoid of microsomal and cytosolic contaminations. *Anal. Biochem.* **287,** 339–342
35. Fujiki, Y., Hubbard, A. L., Fowler, S., and Lazarow, P. B. (1982) Isolation of intracellular membranes by means of sodium carbonate treatment: application to endoplasmic reticulum. *J. Cell Biol.* **93,** 97–102
36. Shevchenko, A., Wilm, M., Vorm, O., and Mann, M. (1996) Mass spectrometric sequencing of proteins silver-stained polyacrylamide gels. *Anal. Chem.* **68,** 850–858
37. Laemmli, U. K. (1970) Cleavage of structural proteins during the assembly of the head of bacteriophage T4. *Nature* **227,** 680–685
38. Neuhoff, V., Arold, N., Taube, D., and Ehrhardt, W. (1988) Improved staining of proteins in polyacrylamide gels including isoelectric focusing gels with clear background at nanogram sensitivity using Coomassie Brilliant Blue G-250 and R-250. *Electrophoresis* **9,** 255–262
39. Gharahdaghi, F., Weinberg, C. R., Meagher, D. A., Imai, B. S., and Mische, S. M. (1999) Mass spectrometric identification of proteins from silver-stained polyacrylamide gel: a method for the removal of silver ions to enhance sensitivity. *Electrophoresis* **20,** 601–605
40. Hauck, S. M., Ekstrom, P. A., Ahuja-Jensen, P., Suppmann, S., Paquet-Durand, F., van Veen, T., and Ueffing, M. (2006) Differential modification of phosducin protein in degenerating rd1 retina is associated with constitutively active Ca^{2+}/calmodulin kinase II in rod outer segments. *Mol. Cell. Proteomics* **5,** 324–336
41. Perkins, D. N., Pappin, D. J., Creasy, D. M., and Cottrell, J. S. (1999) Probability-based protein identification by searching sequence databases using mass spectrometry data. *Electrophoresis* **20,** 3551–3567
42. Pappin, D. J. (1997) Peptide mass fingerprinting using MALDI-TOF mass spectrometry. *Methods Mol. Biol.* **64,** 165–173
43. Towbin, H., Staehelin, T., and Gordon, J. (1979) Electrophoretic transfer of proteins from polyacrylamide gels to nitrocellulose sheets: procedure and some applications. *Proc. Natl. Acad. Sci. U. S. A.* **76,** 4350–4354
44. Palacino, J. J., Sagi, D., Goldberg, M. S., Krauss, S., Motz, C., Wacker, M., Klose, J., and Shen, J. (2004) Mitochondrial dysfunction and oxidative damage in parkin-deficient mice. *J. Biol. Chem.* **279,** 18614–18622
45. Fukada, K., Zhang, F., Vien, A., Cashman, N. R., and Zhu, H. (2004) Mitochondrial proteomic analysis of a cell line model of familial amyotrophic lateral sclerosis. *Mol. Cell. Proteomics* **3,** 1211–1223
46. Graham, J. M., Ford, T., and Rickwood, D. (1990) Isolation of the major subcellular organelles from mouse liver using Nycodenz gradients without the use of an ultracentrifuge. *Anal. Biochem.* **187,** 318–323
47. Malamed, S., and Recknagel, R. O. (1959) The osmotic behavior of the sucrose-inaccessible space of mitochondrial pellets from rat liver. *J. Biol. Chem.* **234,** 3027–3030
48. Dejean, L., Beauvoit, B., Alonso, A. P., Bunoust, O., Guerin, B., and Rigoulet, M. (2002) cAMP-induced modulation of the growth yield of Saccharomyces cerevisiae during respiratory and respiro-fermentative metabolism. *Biochim. Biophys. Acta* **1554,** 159–169
49. Santoni, V., Molloy, M., and Rabilloud, T. (2000) Membrane proteins and proteomics: un amour impossible? *Electrophoresis* **21,** 1054–1070
50. Lodi, T., Alberti, A., Guiard, B., and Ferrero, I. (1999) Regulation of the Saccharomyces cerevisiae DLD1 gene encoding the mitochondrial protein D-lactate ferricytochrome c oxidoreductase by HAP1 and HAP2/3/4/5. *Mol. Gen. Genet.* **262,** 623–632
51. DeRisi, J. L., Iyer, V. R., and Brown, P. O. (1997) Exploring the metabolic and genetic control of gene expression on a genomic scale. *Science* **278,** 680–686
52. Nicholls, D. G., and Ferguson, S. J. (1982) *Bioenergetics 2*, p. 24, Academic Press, London
53. Voet, D., and Voet, J. G. (1990) *Biochemistry*, p. 530, John Wiley, New York, NY
54. Hannig, K., and Heidrich, H. G. (1974) The use of continuous preparative free-flow electrophoresis for dissociating cell fractions and isolation of membranous components. *Methods Enzymol.* **31,** 746–761
55. Zinser, E., and Daum, G. (1995) Isolation and biochemical characterization of organelles from the yeast, Saccharomyces cerevisiae. *Yeast* **11,** 493–536
56. Rapaport, D. (2003) Finding the right organelle. Targeting signals in mitochondrial outer-membrane proteins. *EMBO Rep.* **4,** 948–952
57. Zwizinski, C., Schleyer, M., and Neupert, W. (1984) Proteinaceous receptors for the import of mitochondrial precursor proteins. *J. Biol. Chem.* **259,** 7850–7856
58. Zahedi, R. P., Sickmann, A., Boehm, A. M., Winkler, C., Zufall, N., Schonfisch, B., Guiard, B., Pfanner, N., and Meisinger, C. (2006) Proteomic analysis of the yeast mitochondrial outer membrane reveals accumulation of a subclass of preproteins. *Mol. Biol. Cell* **17,** 1436–1450
59. Janssen, M. J., Koorengevel, M. C., de Kruijff, B., and de Kroon, A. I. (2000) The phosphatidylcholine to phosphatidylethanolamine ratio of Saccharomyces cerevisiae varies with the growth phase. *Yeast* **16,** 641–650
60. Ericson, I. (1974) Determination of the isoelectric point of rat liver mitochondria by cross-partition. *Biochim. Biophys. Acta* **356,** 100–107
61. Hoppe, T., Matuschewski, K., Rape, M., Schlenker, S., Ulrich, H. D., and Jentsch, S. (2000) Activation of a membrane-bound transcription factor by regulated ubiquitin/proteasome-dependent processing. *Cell* **102,** 577–586
62. Ye, Y., Meyer, H. H., and Rapoport, T. A. (2001) The AAA ATPase Cdc48/p97 and its partners transport proteins from the ER into the cytosol. *Nature* **414,** 652–656
63. Dai, R. M., and Li, C. C. (2001)Valosin-containing protein is a multi-ubiquitin chain-targeting factor required in ubiquitin-proteasome degradation. *Nat. Cell Biol.* **3,** 740–744
64. Kiri, A. N., Tran, H. C., Drahos, K. L., Lan, W., McRorie, D. K., and Horn, M. J. (2005) Proteomic changes in bovine heart mitochondria with age: using a novel technique for organelle separation and enrichment. *J. Biomol. Tech.* **16,** 371–379
65. Tulp, A., Verwoerd, D., Fernandez-Borja, M., Neefjes, J., and Hart, A. A. (1996) High resolution density gradient electrophoresis of cellular organelles. *Electrophoresis* **17,** 173–178
66. Tulp, A., Verwoerd, D., and Neefjes, J. (1999) Lectin-induced retardation of subcellular organelles during preparative density gradient electrophoresis: selective purification of plasma membranes. *Electrophoresis* **20,** 438–444
67. Duffy, C. F., Fuller, K. M., Malvey, M. W., O'Kennedy, R., and Arriaga, E. A. (2002) Determination of electrophoretic mobility distributions through the analysis of individual mitochondrial events by capillary electrophoresis with laser-induced fluorescence detection. *Anal. Chem.* **74,** 171–176
68. Fuller, K. M., and Arriaga, E. A. (2004) Capillary electrophoresis monitors changes in the electrophoretic behavior of mitochondrial preparations. *J. Chromatogr. B Anal. Technol. Biomed. Life Sci.* **806,** 151–159
69. Ahmadzadeh, H., Johnson, R. D., Thompson, L., and Arriaga, E. A. (2004) Direct sampling from muscle cross sections for electrophoretic analysis of individual mitochondria. *Anal. Chem.* **76,** 315–321